HHS Public Access

Author manuscript

*Ann Intern Med*. Author manuscript; available in PMC 2025 October 29.

Published in final edited form as:

*Ann Intern Med*. 2025 November ; 178(11): 1561–1570. doi:10.7326/ANNALS-24-01863.

# Association between body composition and cardiometabolic outcomes: a prospective cohort study

**Matthias Jung**[1,2], **Marco Reisert**[3,4], **Hanna Rieder**[1], **Susanne Rospleszcz**[1,5], **Michael T. Lu**[2], **Fabian Bamberg**[1], **Vineet K. Raghu**[2,*], **Jakob Weiss**[1,*]

[1]Department of Diagnostic and Interventional Radiology, University Medical Center Freiburg, Faculty of Medicine, University of Freiburg, Germany

[2]Cardiovascular Imaging Research Center, Department of Radiology, Massachusetts General Hospital and Harvard Medical School, Boston, Massachusetts, USA

[3]Medical Physics, Department of Diagnostic and Interventional Radiology, Medical Center-University of Freiburg, Faculty of Medicine, University of Freiburg, 79106 Freiburg, Germany

[4]Department of Stereotactic and Functional Neurosurgery, Medical Center - University of Freiburg, Faculty of Medicine, University of Freiburg, 79106 Freiburg, Germany

**CORRESPONDING AUTHOR** Matthias Jung, MD, Massachusetts General Hospital, 165 Cambridge St, Suite 400, Boston, MA 02114, mjung6@mgh.harvard.edu; matthias.jung@uniklinik-freiburg.de.

*Drs. Weiss and Raghu jointly supervised this work

AUTHOR CONTRIBUTIONS

**Matthias Jung:** conceptualization, data curation, formal analysis, investigation, methodology, project administration, resources, software, supervision, validation, visualization, writing – original draft

**Marco Reisert:** conceptualization, data curation, formal analysis, methodology, resources, software, supervision, validation, writing – review & editing.

**Hanna Rieder:** data curation, formal analysis, methodology, resources, software, writing – review & editing.

**Susanne Rospleszcz:** conceptualization, data curation, formal analysis, investigation, methodology, project administration, resources, supervision, validation, writing – review & editing.

**Michael T. Lu:** conceptualization, data curation, investigation, methodology, project administration, resources, software, supervision, validation, writing – review & editing.

**Fabian Bamberg:** conceptualization, data curation, funding acquisition, methodology, project administration, resources, software, supervision, validation, writing – review & editing.

**Vineet K. Raghu:** conceptualization, data curation, formal analysis, investigation, methodology, project administration, resources, software, supervision, validation, visualization, writing – original draft

**Jakob Weiss:** conceptualization, data curation, formal analysis, investigation, methodology, project administration, resources, software, supervision, validation, visualization, writing – original draft

ETHICS APPROVAL

Informed consent was obtained from all participants in the UK Biobank.

CONFLICT OF INTEREST

**Matthias Jung:** Research Funding: Deutsche Forschungsgemeinschaft (DFG, German Research Foundation) - 518480401

**Michael T. Lu:** Research funding to his institution: American Heart Association, Astrazeneca, Ionis, Johnson & Johnson Innovation, Kowa, MedImmune, NIH/NHLBI, Risk Management Foundation of the Harvard Medical Institutions Incorporated.

**Fabian Bamberg**: Consulting or Advisory Role: Bayer; Speakers' Bureau: Siemens Healthineers, Bracco Diagnostics, Bayer Health; Research Funding: Siemens Healthineers (Inst), Bayer Health (Inst)

**Vineet K. Raghu:** Research Funding: Norm Group Longevity Impetus Grant, NHLBI K01HL168231, and AHA Career Development Award 935176.

**Jakob Weiss:** Consulting or Advisory Role: Onc.AI; Research Funding: Siemens Healthineers (Inst), Bayer (Inst), Deutsche Forschungsgemeinschaft (DFG, German Research Foundation) – 525002713, National Academy of Medicine, Healthy Longevity Grand Challenge Catalyst Award

REPRODUCIBLE RESEARCH STATEMENT

Protocol: not available.

Statistical Code: Code will be made available via GitHub upon publication.

Data: The data from the UKB needs to be accessed and downloaded upon request in accordance with UKB policies from https://www.ukbiobank.ac.uk. Our body composition measures will be available through https://www.ukbiobank.ac.uk upon publication.

[5]Institute of Epidemiology, Helmholtz Zentrum München, German Research Center for Environmental Health, Neuherberg, Germany

## Abstract

**Background:** Current measures of adiposity have limitations. Artificial intelligence (AI) models may accurately, and efficiently estimate body composition from routine imaging.

**Objective:** To assess the association of AI-derived body composition compartments from magnetic resonance imaging (MRI) with cardiometabolic outcomes.

**Design:** Prospective cohort study.

**Setting:** UK Biobank observational cohort study.

**Participants:** 33,539 UK Biobank participants without a history of diabetes, myocardial infarction, or ischemic stroke (65.0±7.8 years; BMI: 25.8±4.2 kg/$m^2$, 52.8% female) who underwent whole-body MRI.

**Measurements:** An AI tool was applied to MRI to derive 3-dimensional (3D) BC measures, including subcutaneous adipose tissue (SAT), visceral adipose tissue (VAT), skeletal muscle (SM), and SM fat fraction (SMFF), and then calculate their relative distribution. Sex-stratified associations of these relative compartments with incident diabetes mellitus (DM) and major adverse cardiovascular events (MACE) were assessed using restricted cubic splines.

**Results:** Adipose tissue compartments and SMFF increased and SM decreased with age. After adjustment for age, smoking, and hypertension, greater adiposity and lower SM proportion were associated with higher incidence of DM and MACE after a median follow-up of 4.2 years in sex-stratified analyses; however, after additional adjustment for BMI and waist circumference (WC), only elevated VAT proportions and high SMFF were associated with increased risk for DM (respective adjusted hazard ratios [aHRs] for top fifth percentile of the cohort, 2.16 [95% CI, 1.59 to 2.94] and 1.27 [CI, 0.89 to 1.80] in females and 1.84 [CI, 1.48 to 2.27] and 1.84 [CI, 1.43 to 2.37] in males) and MACE (respective aHRs for top fifth percentile of the cohort, 1.37 [CI, 1.00 to 1.88] and 1.72 [CI, 1.23 to 2.41] in females and 1.22 [CI, 0.99 to 1.50] and 1.25 [CI, 0.98 to 1.60] in males). In addition, in males only, low SM proportion was associated with increased risk for DM (aHR for bottom fifth percentile of the cohort, 1.96 [CI, 1.45 to 2.65]) and MACE (aHR, 1.55 [CI, 1.15 to 2.09]).

**Limitations:** Results may not generalize to non-whites or outside the UK.

**Conclusion:** Artificial intelligence–derived BC proportions were strongly associated with cardiometabolic risk, but after BMI and WC were accounted for, only VAT proportion and SMFF (both sexes) and SM proportion (males only) added prognostic information.

**Primary Funding Source:** None.

## INTRODUCTION

Obesity is a global epidemic, estimated to have caused 4 million deaths in 2015, primarily driven by excess cardiometabolic disease(1). 40% of the global population is overweight or obese, and it is projected that >60% of US adults will be obese by 2050(1, 2). Current

obesity definitions rely on body mass index (BMI): >25-<30 for overweight or >30 for obese; however, this conflates excess adiposity with muscle mass and does not account for the location of body fat, critical factors to assess obesity-related cardiometabolic risk(3). Alternative definitions using waist circumference, anthropometric measures, or dual-energy absorptiometry may more directly assess adiposity but still cannot differentiate fat location and distribution (e.g., visceral [VAT] vs subcutaneous adipose tissue [SAT])(4-6).

Cross-sectional scans, such as magnetic resonance imaging (MRI) and computed tomography (CT), are a potential solution to improve adiposity assessment, as their availability is constantly increasing, with an 86% and 127% increase in MRI and CT volume in England over the last decade(7, 8). Despite the well-established link between adiposity and muscle with cardiometabolic and other diseases,(9-11) body composition (BC) measures derived from MRI and CT are not currently quantified in daily practice (9-11). Advances in artificial intelligence have enabled automated, efficient three-dimensional (3D) segmentation of BC compartments, which are more strongly associated with mortality than surrogate 2D areas(12). However, the relationship between imaging-derived BC volumes with cardiometabolic outcomes is unknown.

Here, we used an open-source artificial intelligence model to estimate 3D BC volumes including SAT, VAT, skeletal muscle (SM), and SM fat fraction (SMFF) from whole-body MRIs of >30,000 individuals from the UK Biobank (UKB). We calculated relative adiposity and muscle (e.g., relative SAT is the ratio of SAT to total SAT, VAT, and SM volume) to control for disease-independent factors like sex and height that control total body size (10) (13). Finally, we described age and sex-specific distributions of relative BC compartments across the lifespan and investigated the association between relative BC measures and future cardiometabolic disease risk (diabetes and major adverse cardiovascular events or MACE) beyond BMI, waist circumference, and other traditional risk factors.

## MATERIAL AND METHODS

### Data source

This study used data from the UKB, a large population-based cohort study from the general population(14, 15). Between 2006-2010, 500,000 individuals aged 40-69 (5.5% of invitees) joined the UKB after NHS invitation (16). Although the sampling is likely not representative of the full UK, the large sample size gives credence to exposure-outcome relationships(16).

A subgroup of participants has undergone a panel of imaging exams including MRI. All surviving UKB participants are invited to participate in this substudy, except for those who no longer wish to be contacted or now live outside the UK. The MRI protocol includes a whole-body $T_1$-weighted 3D-VIBE two-point Dixon sequence. Dixon-MRI separates the MRI signals of water and fat, allowing accurate fat and muscle tissue segmentation. Further information is provided in Supplemental Methods. An overview of our study design is provided in Supplemental Figure 1, a flowchart in Supplemental Figure 2.

### Deep learning model and BC measures

We used a validated deep learning (DL) model to measure SAT, VAT, SM (volumes), and SMFF (%) from whole-body MRI (12). In brief, the model was trained on n=150 random participants of the German National Cohort Study (NAKO; whole-body 3-Tesla Dixon-MRI)(17): SAT, VAT, and SM were manually annotated by a radiology resident (5 years of experience in MRI) using a semi-automatic threshold-based 3D segmentation tool in an open-source imaging platform (https://www.nora-imaging.org). Initial segmentations were reviewed by a board-certified attending radiologist (10 years of experience in MR imaging) and flagged if errors were noted. Flagged exams were discussed by consensus between resident and attending, and segmentations were corrected when necessary (minor adjustments in about 10% of cases).

After training, the model was tested on n=50 independent manually segmented NAKO test MRIs not seen during training. These served as ground-truth to assess model performance using Dice scores (measures segmentation accuracy from 0-1: 1 represents perfect overlap between predicted and manual ground-truth segmentations). In our previous study, we reported high agreement between automatic and manual segmentations in the testing dataset, with dice scores of 0.95±0.02 for SAT, 0.92±0.03 for VAT, and 0.93±0.02 for SM (12). We retrained the model using a random sample of n=130 UKB-MRIs, allowing the model to learn nuances (fine-tuning) between the 1.5-Tesla compared to the 3-Tesla Dixon-MRIs used in NAKO. After fine-tuning, we reported dice scores of 0.93±0.01 for SAT, 0.90±0.01 for VAT, and 0.90±0.03 for SM on the UKB testing set (n=50) elsewhere (12).

Here, we provide Bland-Altman-plots to test the model performance in the UKB (Supplemental Figure 3). Bland-Altman plots showed good agreement between manual and deep learning-based segmentations. For SAT, the mean difference was −0.22L (limits of agreement: −1.42L-0.98L), indicating a slight underestimation of SAT (cohort median 14.9L [IQR 11.6-19.3L]; Table 1) by the DL model (Supplemental Figure 3A). VAT had a mean difference of 0.37L, with differences tightly clustered around the mean (limits of agreement: 0.03L-0.72L), reflecting slight overestimation of VAT (cohort median 3.4L [IQR 2.0-5.3L]; Table 1) but strong concordance (Supplemental Figure 3B). Skeletal muscle showed a mean difference of 0.5L, with slightly more variability but overall consistent agreement (limits of agreement: −0.36L-1.36L, Supplemental Figure 3C; cohort mean and standard deviation 11.4±3.0L, Table 1). Sample segmentation results illustrating the model's performance across BMI categories and sex are shown in Supplemental Figure 4.

In addition, we quantified the SM-derived fat fraction (SMFF), a marker of muscle quality that captures metabolically active intramyocellular fat that is not visible macroscopically. SMFF can be estimated from Dixon-MRI, which allows for voxel-wise extraction of water and fat signals, enabling the calculation of a fat fraction (fat signal/[fat+water signal]) from BC segmentation masks. A common drawback of Dixon-MRI is "swap artifacts" where fat signals are misrepresented as water signals, leading to incorrect fat fraction calculations. Swap artifacts occurred in raw scan regions, such as the abdomen, where, e.g., fat was incorrectly displayed as water contrast. When fat and water images were stitched into a whole-body MRI, this swapping caused some regions, e.g., the abdomen, to be displayed incorrectly, e.g., as water contrast, while other regions, e.g., the chest and pelvis,

remained correctly displayed as fat contrast. Therefore, we used a second open-source model to correct for these region-wise swaps in the stitched whole-body MRIs before SMFF quantification, as reported elsewhere(12). Briefly, the model was tested on 180 whole-body MRIs with swaps, and performance was verified by visual review from the radiology resident. All swaps were accurately corrected.

## Outcomes

Primary outcomes were incident diabetes (ICD-10: E10-14; ICD-9: 250) and major adverse cardiovascular events (MACE), defined as myocardial infarction or ischemic stroke (ICD-10: I21-22; I63; I00-I78; ICD-9: 410-411; 433-434), or mortality from major cardiovascular diseases (ICD10: I1-6; I70-78). Outcomes were defined using UKB Data Fields 41270 and 41271 which contain distinct International Classification of Disease 9 and 10 diagnosis codes through linkage to all hospital inpatient records (https://biobank.ctsu.ox.ac.uk/crystal/refer.cgi?id=138483). Mortality from major cardiovascular diseases was extracted through linkage to national death registries (Data-Field 40001). Follow-up time was calculated as the interval between the date of MRI (start and origin time) until earliest date among death, outcome, loss to follow-up, or October 31, 2022 (Censoring date for ICD-based outcomes).

## Covariates

Date of birth, sex, and race were extracted from baseline self-reports. Weight (kg) and height (m) were obtained at the imaging visit. BMI ($kg/m^2$) was categorized as established (BMI<25, healthy weight; BMI=25-29.9, overweight; BMI>30, obese). BMI<18 was included in the healthy weight group due to underrepresentation (n=230). Smoking was categorized into "never", "former," and "current" smokers. Prevalent hypertension was defined as having ICD-10 codes I10-15 or ICD-9 codes 401-405 before the imaging visit. Non-whites (n=1,193, 3% UKB) were excluded due to substantial heterogeneity in the association of BC with disease across ethnic groups. Covariates were identified using a modified disjunctive cause criterion.

## Statistical Analysis

Baseline characteristics are presented as mean ± standard deviation or median with interquartile ranges (IQR) for continuous and absolute counts with percentages for categorical variables.

After automatic extraction of SAT, VAT, and SM, we defined relative BC compartments to adjust for disease-independent contributors to SAT, VAT, and SM volumes (e.g., sex, body size). Relative compartments were defined as the ratio of each measure to the sum of all BC measures, e.g., $SAT_{rel}(\%) = SAT/(SAT+VAT+SM)$. $SAT_{rel}$ of 60% indicates that 60% of a person's total adiposity and muscle is SAT, with the remaining 40% comprising VAT and SM.

Differences in relative BC compartments and SMFF across ages were visualized using density plots.

Outcome analyses were limited to individuals without a history of diabetes, myocardial infarction, or ischemic stroke. To investigate time to outcome, sex-stratified natural cubic splines with 3 knots were computed using the splines package V4.4.2. We calculated sequential models to assess the association between relative BC measures and outcomes: 1) unadjusted model; 2) model adjusted for BMI categories and waist circumference, and 3) model adjusted for BMI categories, waist circumference, prevalent hypertension, and smoking status. Results were additionally reported as adjusted hazard ratios (aHR) and 95% ($2.5^{th}$ and $97.5^{th}$ percentiles) confidence intervals (CI) for the top and bottom 5% and 20% of males and females, respectively. For the underlying sex-stratified Cox models, proportional hazards assumptions were tested by computing scaled Schoenfeld residuals, and linearity was assessed using martingale residuals. Both assumptions were met for all models. Cox regressions were complete case analyses, excluding individuals with one or more missing covariates.

Statistical analyses were performed using R V4.2.2 (R-Core-Team, www.r-project.org, 2024).

### Role of funders

This study received no funding.

## RESULTS

### Study population and BC distribution by age

A total of 33 432 people (17 657 females; mean age, 65.0 years [SD, 7.8]; mean BMI, 25.8 $kg/m^2$ [SD, 4.2]) were included. The Table presents baseline characteristics of included participants. Females had higher SAT and SMFF than males, whereas males had higher SM and VAT ($P < 0.001$ for all; Table).

Across all age groups, SAT was the predominant compartment in females, comprising 58.1% of total BC at age 40 to 49 years and increasing to 60.1% above age 70 years compared with 40.0% and 41.5%, respectively, in males (Figure 1). Skeletal muscle was the predominant compartment in males, peaking at age 40 to 49 years (45.3% in males vs. 35.5% in females) and decreasing thereafter. In both sexes, VAT proportion and SMFF were also higher with increased age.

### Relative BC measures and incident DM and MACE

Over 4.2 years (IQR 3.4-5.6 years), 187/17657 females (1.1%) and 344/15775 males (2.2%) were diagnosed with incident diabetes, and 177/17657 females (1.0%) and 365/15775 males (2.3%) had a major adverse cardiovascular event (MACE). Figures 2 & 3 show results for the sex-stratified association of relative BC measures and future risk for DM and MACE after adjustment for age, smoking status, and hypertension and with additional adjustment for BMI categories and WC.

In models adjusted for age, smoking, and hypertension, greater adiposity measures (SAT proportion, VAT proportion, and SMFF) and low SM proportion were associated with higher incidence of DM and MACE in both sexes (Figures 2 and 3 [upper rows]). These

relationships were consistent with those in unadjusted analyses (Supplement Figures 5 and 6).

After additional adjustment for BMI and WC, the associations between SAT proportion and DM and MACE were attenuated in males (Figure 2 [B] and Figure 3 [B], lower rows), while we observed a negative association between relative SAT and future diabetes risk in females. Females in the bottom 20th percentile of relative SAT (<54.4%) had an aHR of 1.46 (95% CI, 1.23 to 1.72), while females in the top 20th percentile (>64.6%) had an aHR of 0.71 (CI, 0.59 to 0.84) (Figure 2 [A], lower row).

In both sexes, high VAT proportions and high SMFF remained associated with higher risk for DM and MACE. For DM, aHRs for the top fifth percentile were 2.16 (CI, 1.59 to 2.94) and 1.27 (CI, 0.89 to 1.80) in females (Figure 2 [A]) and 1.84 (CI, 1.48 to 2.27) and 1.84 (CI, 1.43 to 2.37) in males (Figure 2 [B]), respectively. For MACE, aHRs were 1.37 (CI, 1.00 to 1.88) and 1.72 (CI, 1.23 to 2.41) in females (Figure 3 [A]) and 1.22 (CI, 0.99 to 1.50) and 1.25 (CI, 0.98 to 1.60) in males (Figure 3 [B]), respectively.

In males only, low SM proportions remained associated with increased risk for DM (aHR for bottom fifth percentile, 1.96 [CI, 1.45 to 2.65]; Figure 2 [B]) and MACE (aHR for bottom fifth percentile, 1.55 [CI, 1.15 to 2.09]; Figure 3 [B]) after adjustment for BMI and WC.

Results were consistent across BMI subgroups (Supplemental Figures 7-9).

## DISCUSSION

Excess adiposity is a key driver of cardiometabolic disease, but current definitions of obesity rely on BMI, an accessible but poor surrogate (3). Here, we applied an artificial intelligence segmentation tool to whole-body MRIs from >30,000 UK Biobank participants to extract 3D BC compartments, including subcutaneous adipose tissue (SAT), visceral adipose tissue (VAT), skeletal muscle (SM), and skeletal muscle fat fraction (SMFF). We found that the tool accurately extracted 3D BC volumes from whole-body MRIs in <3 minute per scan. We then used these measures to describe how relative proportions of each compartment change across the lifespan. We found that as both sexes age, adipose tissue compartments and myosteatosis (SMFF) increases while SM decreases. Lastly, we found that high VAT proportions and myosteatosis were associated with incident diabetes risk in both sexes, low SM was associated with higher risk in males, and SAT proportions were not associated with higher risk in either sex. We found similar but weaker associations with incident cardiovascular events, and all associations were robust to adjustment for BMI, waist circumference, and clinical risk factors.

These results corroborate evidence that VAT, but not SAT, is a key driver of adiposity-related cardiometabolic risk (18-20). We also confirm findings that ectopic fat in the muscle leads to insulin resistance and cardiovascular risk (21, 22). Contrary to emerging evidence, we found that low skeletal muscle proportions were more strongly associated with cardiometabolic risk in men than in women (23). Counterintuitively, we noted a small protective effect of high SAT proportion and volume in women after adjustment for waist circumference. SAT may confer metabolic protection compared to visceral fat, particularly in women (24, 25),

and thus may serve as a proxy for low visceral adiposity. However, we did not observe this protective effect for cardiovascular outcomes, and it may also reflect residual confounding. (26)

BMI has known limitations and is only recommended as a population-based measure for epidemiological studies or as a screening tool (3). Cardiometabolic disease guidelines suggest more direct measurement of adiposity using anthropometric metrics like waist circumference and waist-to-hip ratio or dual-energy x-ray absorptiometry (27, 28). These measures are more closely related to abdominal adiposity than BMI but are unable to assess relative BC proportions (correlation to VAT/SAT ratio~0.1), suggesting that they may be proxies of total adiposity/size (29). The model used in this study enables direct measurement of BC compartments and relative proportions, which are shown here to be associated with cardiometabolic risk beyond BMI and waist circumference.

The benefit of anthropometric metrics are their ease of use. Whole-body MRI is becoming increasingly popular as a direct-to-consumer screening tool but is not performed in clinical routine. Though we do not recommend specifically ordering whole-body MRIs to assess BC, a pragmatic clinical implementation may be an opportunistic screening strategy, where BC data is automatically extracted from routine clinical MRI or CT scans, regardless of their initial indication. A critical next step towards this paradigm is to test whether BC proportions extracted from common clinical scan regions (liver, kidney, etc.) produce similar estimates as our whole-body approach. If successful, this model could be implemented in the Electronic Medical Record (EMR) without disrupting established workflows to automatically quantify potentially prognostic body composition measurements from routine MRIs or CTs that would otherwise be missed. Our model was trained on a $T_1$-weighted Dixon sequence, which is widely used in daily routine and comparable to other commonly used $T_1$-weighted sequences (30).

Growing evidence suggests that BC plays a key role not only in cardiometabolic but also oncologic diseases to personalize risk estimation (31-33). In addition, BC could also play a crucial role in estimating treatment tolerability and the risk of treatment-related toxicity. In this context, beyond defining excess adiposity, our DL model and relative BC profiles could be used as a frailty or overall health measure to improve treatment decisions for accurate, personalized dosing of systemic drug therapies, including chemotherapy and immunotherapy (33-35).

This study has limitations. First, the study population is non-Hispanic white adults >45 years old and the results may not generalize to other demographic groups (16). A major challenge in obesity management is that BMI and waist circumference require specific thresholds and have variable accuracy to identify excess adiposity in individuals of different race/ethnicity. MRI has potential to address this issue with direct measurement of BC (36); however, further testing is needed to determine whether the DL-model generalizes to diverse populations. We did not assess test-retest reliability of the DL segmentations here; however, Bland-Altman analysis showed that DL-segmentations were robust despite the rather small testing cohort. Third, Dixon-swap artifacts are common errors in clinical routine, meaning that a fat-only signal can be erroneously displayed in parts where a water-only signal

is expected, resulting in incorrect Dixon-derived SMFF calculations (37, 38). While we corrected swap-artifacts in our study before SMFF extraction, this may be a barrier to the translation of SMFF into practice. Furthermore, future studies need to investigate whether the model generalizes to non-Siemens scans and different field-strengths. Fourth, granular information on smoking history (e.g., pack-years), physical activity, and socioeconomic status was not available for most of our cohort and may introduce residual confounding. Last, we used thoracoabdominal SAT, VAT, and SM to define thresholds; however, fat location (e.g. ectopic or gluteofemoral fat) may play different roles in conferring cardiometabolic risk. Future studies will focus on anatomic region-specific measurements to further refine our high-risk definition and improve its clinical utility.

In conclusion, automated MRI-based body composition analysis is accurate and feasible. Automated body composition measurements are associated with cardiometabolic risk beyond BMI, waist circumference, and traditional risk factors. Upon further validation in diverse populations, this approach may enable opportunistic assessment of body composition from routine imaging to identify patients at high cardiometabolic risk.

## Supplementary Material

Refer to Web version on PubMed Central for supplementary material.

## ACKNOWLEDGMENTS

This research has been conducted using the UK Biobank Resource under Application Number 80337. We thank all participants who took part in the NAKO and UKB study and the staff of these research initiatives. MJ was supported by the Deutsche Forschungsgemeinschaft (DFG, German Research Foundation) - 518480401. VKR was supported by Norn Group Longevity Impetus Grant, NHLBI K01HL168231, and AHA Career Development Award 935176.

### PRIMARY FUNDING SOURCE

There was no primary funding source for this study.

## REFERENCES

1. Collaborators GBDO, Afshin A, Forouzanfar MH, Reitsma MB, Sur P, Estep K, et al. Health Effects of Overweight and Obesity in 195 Countries over 25 Years. N Engl J Med. 2017;377(1):13–27. [PubMed: 28604169]
2. Collaborators GUOF. National-level and state-level prevalence of overweight and obesity among children, adolescents, and adults in the USA, 1990-2021, and forecasts up to 2050. Lancet. 2024;404(10469):2278–98. [PubMed: 39551059]
3. Rubino F, Cummings DE, Eckel RH, Cohen RV, Wilding JPH, Brown WA, et al. Definition and diagnostic criteria of clinical obesity. Lancet Diabetes Endocrinol. 2025.
4. Shepherd JA, Ng BK, Sommer MJ, Heymsfield SB. Body composition by DXA. Bone. 2017;104:101–5. [PubMed: 28625918]
5. Ross R, Neeland IJ, Yamashita S, Shai I, Seidell J, Magni P, et al. Waist circumference as a vital sign in clinical practice: a Consensus Statement from the IAS and ICCR Working Group on Visceral Obesity. Nat Rev Endocrinol. 2020;16(3):177–89. [PubMed: 32020062]
6. Agrawal S, Klarqvist MDR, Diamant N, Stanley TL, Ellinor PT, Mehta NN, et al. BMI-adjusted adipose tissue volumes exhibit depot-specific and divergent associations with cardiometabolic diseases. Nat Commun. 2023;14(1):266. [PubMed: 36650173]

7. England NHS;Pageshttps://www.england.nhs.uk/statistics/statistical-work-areas/diagnostic-imaging-dataset/diagnostic-imaging-dataset-2012-13-data-2/ on June 24th 2024.
8. England NHS;Pageshttps://www.england.nhs.uk/statistics/statistical-work-areas/diagnostic-imaging-dataset/diagnostic-imaging-dataset-2023-24-data/ on June 24th 2024.
9. Thomas EL, Bell JD. Influence of undersampling on magnetic resonance imaging measurements of intra-abdominal adipose tissue. Int J Obes Relat Metab Disord. 2003;27(2):211–8. [PubMed: 12587001]
10. Shen W, Chen J, Gantz M, Velasquez G, Punyanitya M, Heymsfield SB. A single MRI slice does not accurately predict visceral and subcutaneous adipose tissue changes during weight loss. Obesity (Silver Spring). 2012;20(12):2458–63. [PubMed: 22728693]
11. Faron A, Luetkens JA, Schmeel FC, Kuetting DLR, Thomas D, Sprinkart AM. Quantification of fat and skeletal muscle tissue at abdominal computed tomography: associations between single-slice measurements and total compartment volumes. Abdom Radiol (NY). 2019;44(5):1907–16. [PubMed: 30694368]
12. Jung M, Raghu VK, Reisert M, Rieder H, Rospleszcz S, Pischon T, et al. Deep learning-based body composition analysis from whole-body magnetic resonance imaging to predict all-cause mortality in a large western population. EBioMedicine. 2024;110:105467. [PubMed: 39622188]
13. Derstine BA, Holcombe SA, Ross BE, Wang NC, Su GL, Wang SC. Optimal body size adjustment of L3 CT skeletal muscle area for sarcopenia assessment. Sci Rep. 2021;11(1):279. [PubMed: 33431971]
14. Sudlow C, Gallacher J, Allen N, Beral V, Burton P, Danesh J, et al. UK biobank: an open access resource for identifying the causes of a wide range of complex diseases of middle and old age. PLoS Med. 2015;12(3):e1001779. [PubMed: 25826379]
15. Bamberg F, Kauczor HU, Weckbach S, Schlett CL, Forsting M, Ladd SC, et al. Whole-Body MR Imaging in the German National Cohort: Rationale, Design, and Technical Background. Radiology. 2015;277(1):206–20. [PubMed: 25989618]
16. Littlejohns TJ, Holliday J, Gibson LM, Garratt S, Oesingmann N, Alfaro-Almagro F, et al. The UK Biobank imaging enhancement of 100,000 participants: rationale, data collection, management and future directions. Nat Commun. 2020;11(1):2624. [PubMed: 32457287]
17. German National Cohort C The German National Cohort: aims, study design and organization. Eur J Epidemiol. 2014;29(5):371–82. [PubMed: 24840228]
18. Shulman GI. Ectopic fat in insulin resistance, dyslipidemia, and cardiometabolic disease. N Engl J Med. 2014;371(12):1131–41. [PubMed: 25229917]
19. Koh H, Hayashi T, Sato KK, Harita N, Maeda I, Nishizawa Y, et al. Visceral adiposity, not abdominal subcutaneous fat area, is associated with high blood pressure in Japanese men: the Ohtori study. Hypertens Res. 2011;34(5):565–72. [PubMed: 21228782]
20. Porter SA, Massaro JM, Hoffmann U, Vasan RS, O'Donnel CJ, Fox CS. Abdominal subcutaneous adipose tissue: a protective fat depot? Diabetes Care. 2009;32(6):1068–75. [PubMed: 19244087]
21. Souza A, Troschel AS, Marquardt JP, Hadzic I, Foldyna B, Moura FA, et al. Skeletal muscle adiposity, coronary microvascular dysfunction, and adverse cardiovascular outcomes. Eur Heart J. 2025.
22. Goodpaster BH, Bergman BC, Brennan AM, Sparks LM. Intermuscular adipose tissue in metabolic disease. Nat Rev Endocrinol. 2023;19(5):285–98. [PubMed: 36564490]
23. Diaz-Canestro C, Pentz B, Sehgal A, Yang R, Xu A, Montero D. Lean body mass and the cardiovascular system constitute a female-specific relationship. Sci Transl Med. 2022;14(667):eabo2641. [PubMed: 36260693]
24. Golan R, Shelef I, Rudich A, Gepner Y, Shemesh E, Chassidim Y, et al. Abdominal superficial subcutaneous fat: a putative distinct protective fat subdepot in type 2 diabetes. Diabetes Care. 2012;35(3):640–7. [PubMed: 22344612]
25. Chen P, Hou X, Hu G, Wei L, Jiao L, Wang H, et al. Abdominal subcutaneous adipose tissue: a favorable adipose depot for diabetes? Cardiovasc Diabetol. 2018;17(1):93. [PubMed: 29945626]
26. Chait A, den Hartigh LJ. Adipose Tissue Distribution, Inflammation and Its Metabolic Consequences, Including Diabetes and Cardiovascular Disease. Front Cardiovasc Med. 2020;7:22. [PubMed: 32158768]

27. American Diabetes Association Professional Practice C. 8. Obesity and Weight Management for the Prevention and Treatment of Type 2 Diabetes: Standards of Care in Diabetes-2024. Diabetes Care. 2024;47(Suppl 1):S145–S57. [PubMed: 38078578]

28. Powell-Wiley TM, Poirier P, Burke LE, Despres JP, Gordon-Larsen P, Lavie CJ, et al. Obesity and Cardiovascular Disease: A Scientific Statement From the American Heart Association. Circulation. 2021;143(21):e984–e1010. [PubMed: 33882682]

29. Klarqvist MDR, Agrawal S, Diamant N, Ellinor PT, Philippakis A, Ng K, et al. Silhouette images enable estimation of body fat distribution and associated cardiometabolic risk. NPJ Digit Med. 2022;5(1):105. [PubMed: 35896726]

30. Salari R, Ballard DH, Hoegger MJ, Young D, Shetty AS. Fat-only Dixon: how to use it in body MRI. Abdom Radiol (NY). 2022;47(7):2527–44. [PubMed: 35583822]

31. Bates DDB, Pickhardt PJ. CT-Derived Body Composition Assessment as a Prognostic Tool in Oncologic Patients: From Opportunistic Research to Artificial Intelligence-Based Clinical Implementation. AJR Am J Roentgenol. 2022;219(4):671–80. [PubMed: 35642760]

32. DeFreitas MR, Toronka A, Nedrud MA, Cubberley S, Zaki IH, Konkel B, et al. CT-derived body composition measurements as predictors for neoadjuvant treatment tolerance and survival in gastroesophageal adenocarcinoma. Abdom Radiol (NY). 2023;48(1):211–9. [PubMed: 36209446]

33. Cespedes Feliciano EM, Chen WY, Lee V, Albers KB, Prado CM, Alexeeff S, et al. Body Composition, Adherence to Anthracycline and Taxane-Based Chemotherapy, and Survival After Nonmetastatic Breast Cancer. JAMA Oncol. 2020;6(2):264–70. [PubMed: 31804676]

34. Falsarella GR, Gasparotto LP, Barcelos CC, Coimbra IB, Moretto MC, Pascoa MA, et al. Body composition as a frailty marker for the elderly community. Clin Interv Aging. 2015;10:1661–6. [PubMed: 26527868]

35. Griggs JJ, Bohlke K, Balaban EP, Dignam JJ, Hall ET, Harvey RD, et al. Appropriate Systemic Therapy Dosing for Obese Adult Patients With Cancer: ASCO Guideline Update. J Clin Oncol. 2021;39(18):2037–48. [PubMed: 33939491]

36. Rao G, Powell-Wiley TM, Ancheta I, Hairston K, Kirley K, Lear SA, et al. Identification of Obesity and Cardiovascular Risk in Ethnically and Racially Diverse Populations: A Scientific Statement From the American Heart Association. Circulation. 2015;132(5):457–72. [PubMed: 26149446]

37. Kirchgesner T, Acid S, Perlepe V, Lecouvet F, Vande Berg B. Two-point Dixon fat-water swapping artifact: lesion mimicker at musculoskeletal T2-weighted MRI. Skeletal Radiol. 2020;49(12):2081–6. [PubMed: 32556469]

38. Haueise T, Schick F, Stefan N, Schlett CL, Weiss JB, Nattenmuller J, et al. Analysis of volume and topography of adipose tissue in the trunk: Results of MRI of 11,141 participants in the German National Cohort. Sci Adv. 2023;9(19):eadd0433. [PubMed: 37172093]

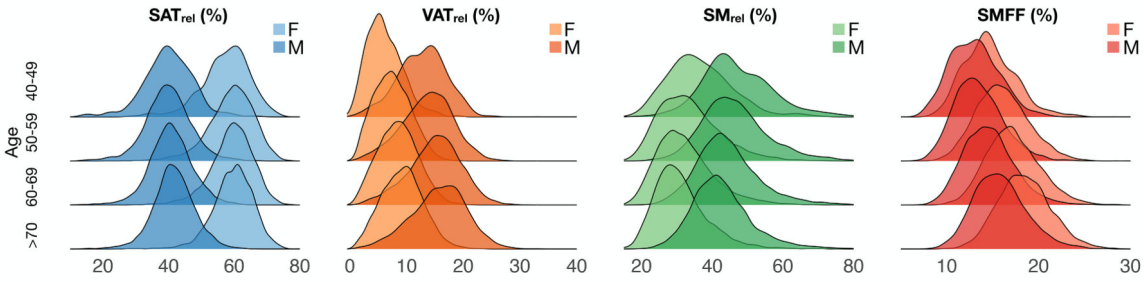


| Age, y | Female SAT$_{rel}$ (%) (Q1-Q3) | Male SAT$_{rel}$ (%) (Q1-Q3) | Female VAT$_{rel}$ (%) (Q1-Q3) | Male VAT$_{rel}$ (%) (Q1-Q3) | Female SM$_{rel}$ (%) (Q1-Q3) | Male SM$_{rel}$ (%) (Q1-Q3) | Female SMFF (%) (Q1-Q3) | Male SMFF (%) (Q1-Q3) |
|---|---|---|---|---|---|---|---|---|
| 40-49 | 58.1 (53.5-62.4) | 40.0 (35.7-44.8) | 5.6 (3.8-8.0) | 13.1 (10.0-15.5) | 35.5 (30.2-41.7) | 45.3 (40.7-53.3) | 14.5 (12.8-16.3) | 12.9 (11.1-14.6) |
| 50-59 | 59.7 (55.1-63.8) | 39.9 (35.6-44.1) | 7.3 (5.0-9.8) | 13.9 (10.7-16.8) | 32.4 (27.1-38.3) | 45.4 (40.1-51.5) | 15.8 (14.0-17.9) | 13.2 (11.5-15.1) |
| 60-69 | 59.8 (55.6-63.6) | 40.6 (36.7-44.7) | 8.4 (6.0-10.9) | 15.2 (12.1-18.1) | 31.2 (26.5-36.6) | 43.2 (38.4-48.9) | 17.0 (15.2-19.0) | 14.4 (12.6-16.3) |
| >70 | 60.1 (56.1-63.8) | 41.5 (37.9-45.5) | 9.3 (6.6-11.7) | 16.0 (12.6-19.0) | 29.9 (25.8-34.9) | 41.7 (36.9-47.2) | 18.4 (16.5-20.3) | 15.6 (13.8-17.6) |

**Figure 1: Change in relative body composition across age in decades**

Density plots illustrate the change in relative body composition measures SAT$_{rel}$ (blue), VAT$_{rel}$ (orange), SM$_{rel}$ (green), and SMFF (red) across age decades. While there is an increase in relative adipose tissue volume (SAT$_{rel}$, VAT$_{rel}$) across age decades, there is a decrease in SM$_{rel}$ accompanied by an increase in SMFF. Sex-stratified median (IQR) relative body composition measures are provided in the tables below the plots.

IQR, interquartile range. SAT, subcutaneous adipose tissue. SM, skeletal muscle. SMFF, skeletal muscle fat fraction. VAT, visceral adipose tissue. rel, body composition measure relative to the sum of all body composition measures

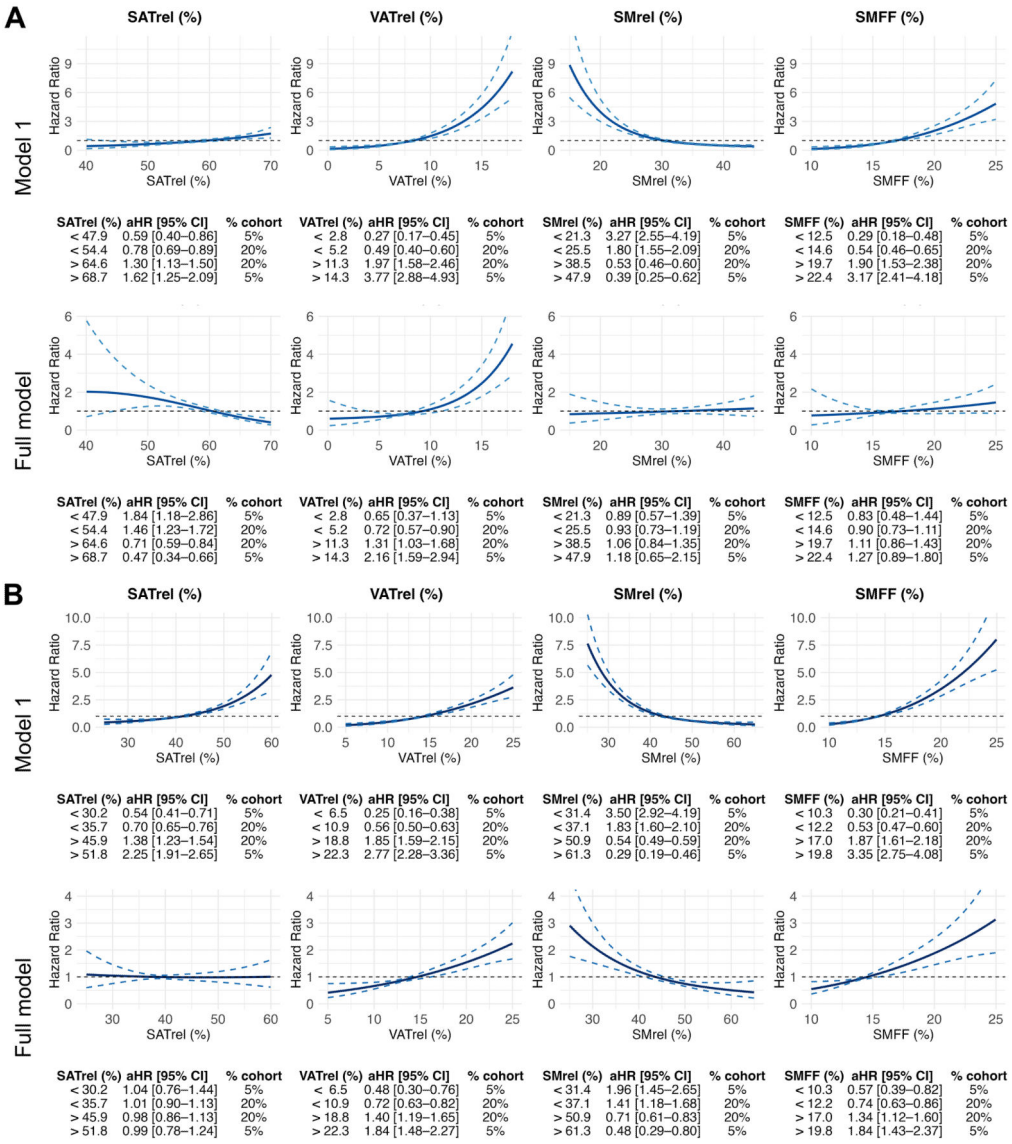


**Figure 2: Multivariable adjusted spline curves for incident diabetes**

Sex-stratified multivariable adjusted spline plots (**A**, females; **B**, males) show the relationship between relative body composition measures and incident diabetes risk. The tables below each graph show the adjusted hazard ratios (HRs) and 95% confidence intervals (CIs) for the bottom and top 5% and 20% of the cohort. Dashed lines, 95% confidence interval. The models are adjusted for age, BMI categories, waist circumference, prevalent hypertension, and smoking status.

CI, confidence interval. SAT, subcutaneous adipose tissue. SM, skeletal muscle. SMFF, skeletal muscle fat fraction. VAT, visceral adipose tissue. rel, body composition measure relative to the sum of all body composition measures

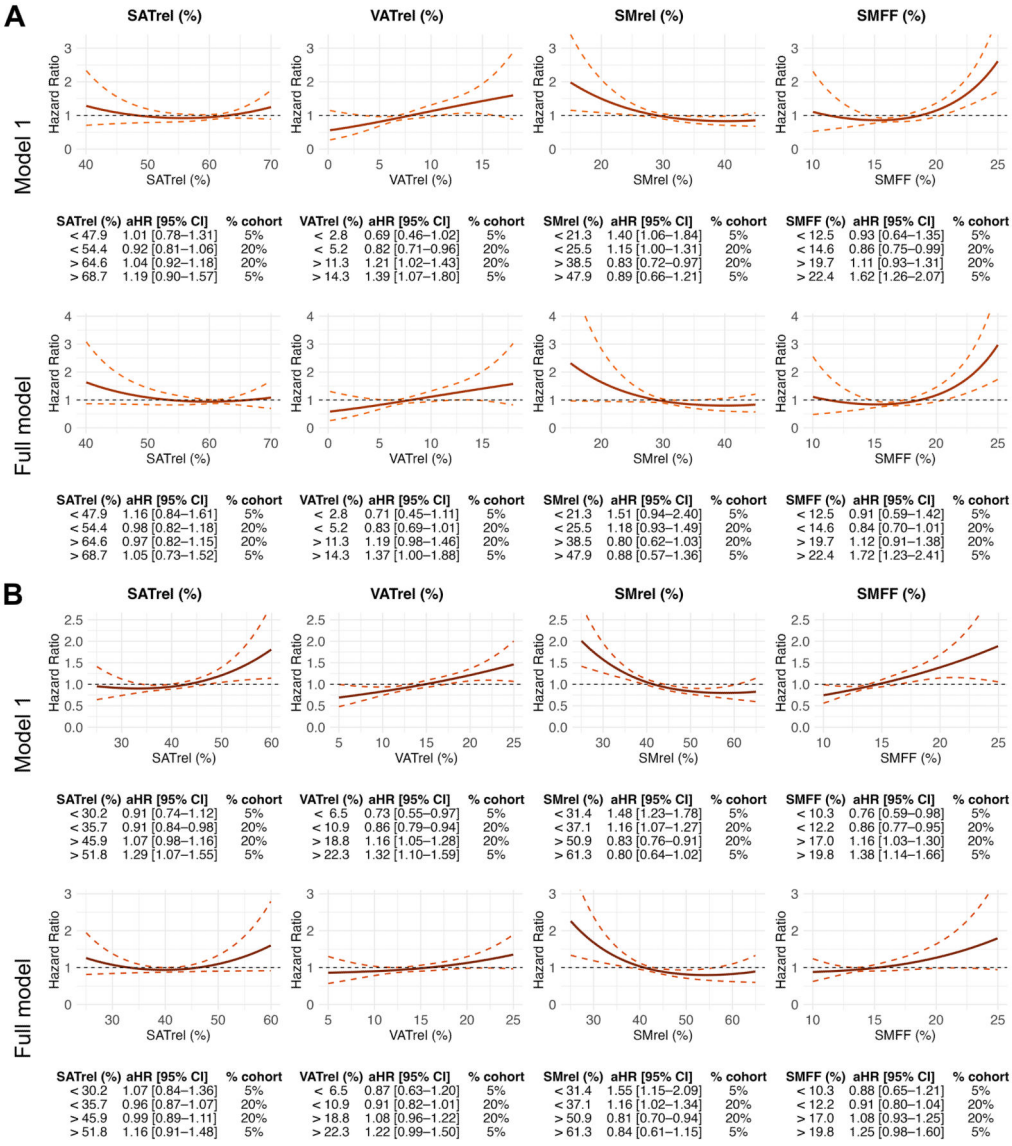


**Figure 3: Multivariable adjusted spline curves for incident MACE**

Sex-stratified multivariable adjusted spline plots (**A**, females; **B**, males) show the relationship between relative body composition measures and incident MACE risk. The tables below each graph show the adjusted hazard ratios (HRs) and 95% confidence intervals (CIs) for the bottom and top 5% and 20% of the cohort. Dashed lines, 95% confidence interval. The models are adjusted for age, BMI categories, waist circumference, prevalent hypertension, and smoking status.

CI, confidence interval. SAT, subcutaneous adipose tissue. SM, skeletal muscle. SMFF, skeletal muscle fat fraction. VAT, visceral adipose tissue. rel, body composition measure relative to the sum of all body composition measures

**Table 1: Cohort characteristics**

| Characteristic | Overall, N = 33,432 | Female, N = 17,657 | Male, N = 15,775 |
|---|---|---|---|
| **Age, y** | | | |
| Mean ± SD | 65.0 ± 7.8 | 64.4 ± 7.6 | 65.6 ± 7.9 |
| Median (IQR) | 65.4 (59.0, 71.0) | 64.6 (58.5, 70.3) | 66.4 (59.6, 71.8) |
| **BMI, n (%)** | | | |
| **< *25* kg/m$^2$** | 16,022 (48%) | 9,708 (55%) | 6,314 (40%) |
| ***25-29.9* kg/m$^2$** | 12,657 (38%) | 5,474 (31%) | 7,183 (46%) |
| **≥ *30* kg/m$^2$** | 4,753 (14%) | 2,475 (14%) | 2,278 (14%) |
| **Waist circumference, cm** | | | |
| Mean ± SD | 88.1 ± 12.5 | 82.6 ± 11.6 | 94.2 ± 10.5 |
| Median (IQR) | 88.0 (79.0, 96.0) | 81.0 (74.0, 90.0) | 93.0 (87.0, 100.0) |
| **SAT, L** | | | |
| Median (IQR) | 14.9 (11.6, 19.3) | 17.0 (13.4, 21.6) | 13.0 (10.4, 16.3) |
| **VAT, L** | | | |
| Median (IQR) | 3.4 (2.0, 5.3) | 2.4 (1.4, 3.6) | 5.0 (3.4, 6.6) |
| **SM, L** | | | |
| Mean ± SD | 11.4 ± 3.0 | 9.1 ± 1.3 | 14.0 ± 2.1 |
| **SMFF, %** | | | |
| Mean ± SD | 16.0 ± 3.2 | 17.1 ± 3.0 | 14.7 ± 2.9 |
| **History of Hypertension, n (%)** | 4,293 (13%) | 1,852 (10%) | 2,441 (15%) |
| **Smoking status**** **, n (%)** | | | |
| ***never*** | 15,431 (47%) | 8,671 (50%) | 6,760 (43%) |
| ***former*** | 17,023 (51%) | 8,478 (49%) | 8,545 (55%) |
| ***current*** | 634 (1.9%) | 297 (1.7%) | 337 (2.2%) |
| **Incident Diabetes** | 531 (1.6%) | 187 (1.1%) | 344 (2.2%) |
| **Incident MACE** | 542 (1.6%) | 177 (1.0%) | 365 (2.3%) |
| **Follow up time, y** | | | |
| Mean ± SD | 4.5 ± 1.8 | 4.5 ± 1.8 | 4.4 ± 1.8 |
| Median (IQR) | 4.2 (3.3, 5.6) | 4.2 (3.4, 5.6) | 4.2 (3.3, 5.5) |

** n=33088 for smoking status

BMI, body mass index. L, liters SAT, subcutaneous adipose tissue. SM, skeletal muscle. SMFF, skeletal muscle fat fraction. VAT, visceral adipose tissue. Y, years